MMP Inhibition Blocks Fibroblast-dependent Skin Cancer Invasion, Reduces Vascularization and Alters VEGF-A and PDGF-BB Expression

EVA C. WOENNE[1*], WILTRUD LEDERLE[2*], STEFAN ZWICK[1], MORITZ PALMOWSKI[2], HANS KRELL[3], WOLFHARD SEMMLER[1], MARGARETA M. MUELLER[4] and FABIAN KIESSLING[2]

[1]*Department of Medical Physics in Radiology, and* [4]*Tumor and Microenvironment Group, German Cancer Research Center, INF 280, D-69120 Heidelberg, Germany;*
[2]*Department of Experimental Molecular Imaging, Medical Faculty, RWTH Aachen University, D-52074 Aachen, Germany;*
[3]*Pharma Research Penzberg, Roche Diagnostics GmbH, D-82377 Penzberg, Germany*

Abstract. *Tumor invasion requires intense interactions with stromal cells and a profound extracellular matrix remodelling by matrix metalloproteinases (MMPs). Here, we assessed the specific contribution of fibroblasts to tumor invasion, MMPs, tissue inhibitors of MMPs and angiogenesis-related cytokine expression in organotypic cultures of highly malignant HaCaT-ras A-5RT3 cells, with and without MMP inhibition. Collagen degradation, the hallmark of tumor invasion, was dependent on fibroblasts and active MMP-2. Additionally, MMP blockade down-regulated VEGF-A and up-regulated PDGF-BB. These results were paralleled in xenotransplants in vivo, demonstrating strong inhibitory effects of MMP blockade on tumor invasion and vascularization, as shown by the almost complete absence of VEGF-A and MMP-14 and by the decrease in relative blood volume. MMP blockade also increased the fraction of mature vessels, as demonstrated by an increased mean tumor vessel diameter and a higher ratio of Ng2-positive vessels. Thus, this study highlights the importance of targeting the tumor stroma to defeat cancer.*

Tumor growth, invasion and metastasis strongly depend on a reactive stroma (1, 2). Tumor-associated stromal cells such as fibroblasts can promote tumorigenic conversion of preneoplastic cells by producing cytokines, chemokines and proteases (3, 4), resulting in the remodelling of the adjacent extracellular matrix (ECM) (1). Tumor-associated fibroblasts secrete the proangiogenic vascular endothelial growth factor (VEGF) that stimulates blood vessel sprouting and increases vessel permeability (5). Stabilization of the newly formed vasculature is mainly mediated by platelet-derived growth factor-BB (PDGF-BB), one of the most important chemoattractants and mitogens for smooth muscle cells, pericytes and fibroblasts (6). PDGF is expressed by tumor and stromal cells (7) and can regulate VEGF expression and secretion in fibroblasts (6). Matrix metalloproteinases (MMPs), particularly the gelatinases MMP-2 and MMP-9, play a significant role in ECM remodelling (8, 9) during angiogenesis (10) and tumor invasion since they efficiently degrade the basement membrane (BM) (11). MMP-2 is expressed by fibroblasts, keratinocytes, endothelial and tumor cells, and MMP-9 is produced by keratinocytes, monocytes, macrophages and tumor cells. MMPs are activated by cleavage of the inactive pro-enzymes and are regulated by naturally occurring tissue inhibitors, the TIMPs. More specifically, MMP-2 can be activated by MMP-14 in the presence of TIMP-2 (11).

Previous studies have demonstrated that MMP inhibition is capable of reducing tumor growth, angiogenesis and invasion. Since the efficacy of broad-spectrum MMP inhibitors in defeating tumor growth was shown to be limited, new MMP inhibitors with a higher specificity and selectivity have been developed (12). However, most of them still target more than one MMP. The MMP inhibitor Prinomastat (Ag3340) predominantly targets MMP-2/-9, but also MMP-1, MMP-13 and MMP-14 with lower affinity (13). The MMP-inhibitor Ro28-2653 belongs to a group of novel pyrimidine-2,4,6-trion-based MMP-inhibitors (13, 14) and has a high selectivity for MMP-2/-9, MMP-14 and MMP-8 (14).

In this study, using three-dimensional organotypic cultures (OTCs), we investigated collagen degradation, a hallmark of

*These Authors equally contributed to this work.

Correspondence to: Professor Dr. Fabian Kiessling, Department of Experimental Molecular Imaging, Medical Faculty, RWTH Aachen University, D-52074 Aachen, Germany. Tel: +49 2418080116, Fax: +49 241803380116, e-mail: fkiessling@ukaachen.de

Key Words: Fibroblast, MMP inhibition, angiogenesis, cytokine, imaging.

tumor invasion, in relation to MMP-1, MMP-2, MMP-9, TIMP-1 and TIMP-2. The effect of inhibition of MMPs in OTCs with Ag3340 on tumor invasion was investigated. Non-invasive imaging of tumors by high frequency ultrasound (US) and magnetic resonance imaging (MRI) supported by immunohistological analyses was used to assess tumor vascularization.

Materials and Methods

In vitro three-dimensional OTCs. Cultivation of the highly malignant keratinocyte cell line HaCaT-ras A-5RT3 and preparation of three-dimensional OTCs were performed as described previously (15, 16). In brief, dermal equivalents either containing 2.5×10^5 human dermal fibroblasts or without fibroblasts were prepared with native type I rat collagen (final concentration of 3 mg/ml). Tumor cells (1×10^6 of HaCaT-ras A-5RT3 were plated on top. After 24 hours, cultures were raised to the air-medium interface by lowering the medium level. OTCs were treated with an MMP inhibitor (Ro28-2653) or with solvent (dimethyl sulfoxide, DMSO) alone. Treatment was performed from days 5 to 21 of culture with a concentration of 20 mM of *Ro28-2653* with every medium change. Treated and untreated cultures were harvested on day 7, 14 and 21 after collection of conditioned media and processed for immunohistological analyses. Stained tissue sections of OTCs were viewed using a Leica microscope (DMRE, Bensheim, Germany) and quantitatively analysed as mentioned elsewhere (6).

ELISA of conditioned media. Human MMP-1 (DMP100), human MMP-2 (DMP200), human MMP-9 (DMP900), human TIMP-1 (DTM 100), human TIMP-2 (DTM200), human VEGF-A (DVE00) and human PDGF-BB (DBB00) (all R&D Systems Wiesbaden, Germany) were determined in conditioned media on days 7, 14 and 21 by ELISA according to the manufacturer's instructions. The amount of the respective protein per ml conditioned medium was normalized to the cell density determined on a histological section of the age-matched OTC at its maximal extension. This was done to account for variations in the cell density between different OTCs and for the increase in cell number over time.

Reverse transcriptase-polymerase chain reaction (RT-PCR) analysis. mRNA was isolated using RNeasy mini kit (Qiagen, Hilden, Germany). Reverse transcription and PCR were performed as described elsewhere (6) with the following primer sequences and annealing temperatures: MMP-1 forward: 5-CTC CAC TGC TGC TGC TGC TGT-3, MMP-1 reverse: 5-CAT CTG GGC TGC TTC ATC ACC TTC-3, 65˚C annealing temperature; MMP-2 forward: 5-CGC AGT GAC GGA AAG ATG TGG T-3, MMP-2 reverse: 5-TGG GAT TGG AGG GGG AGG G-3, 65˚C annealing temperature; MMP-9 reverse: 5-TGC TGG GCT GCT GCT TTG CT-3, MMP-9 forward: 5-CGG TCG TCG GTG TCG TAG TTG G-3, 65˚C annealing temperature; TIMP-1 forward: 5-GGG GAC ACC AGA AGT CAA CCA GAC-3, TIMP-1 reverse: 5-GAA GCC CTT TTC AGA GCC TTG GAG-3, 60˚C annealing temperature; TIMP-2 forward: 5-TGG AAA CGA CAT TTA TGG CAA CC-3, TIMP-2 reverse: 5-ACA GGA GCC GTC ACT TCT CTT GAT-3, 65˚C annealing temperature; glyceraldehyde-3-phosphate dehydrogenase GAPDH reverse: 5-GAG GGA TCT CGC TCC TGG AAG A-3, 60˚C annealing temperature; GAPDH reverse: 5-CAG TGG GGA CAC GGA AGG-3, 60˚C annealing temperature.

Tumorigenicity assays in vivo. All experiments were approved by the Governmental Review Committee on Animal Care. HaCaT-ras A-5RT3 tumors were initiated by subcutaneous (*s.c.*) injection (17, 18).

Examination protocol. A total of 14 nude mice with SCCs were examined using US, starting on day 21 after *s.c.* injection of tumor cells. After the US examination, animals received either 110 μl MMP inhibitor Ag3340 (Prinomastat, 150 mg/kg twice a day, *i.p.* for 6 days; n=7) or 110 μl NaCl solution (twice a day, *i.p.* for 6 days; control group, n=7). After 6 days, US examination was repeated. MRI of treated and untreated animals was only performed at the second time point. Gas anaesthesia was used in all non-invasive imaging experiments (17, 18).

Vessel size imaging (VSI) with MRI. MRI was performed using a clinical 1.5 T whole-body MRI system (Siemens Magnetom Vision, Erlangen, Germany) using a custom-made radiofrequency (rf) coil ('animal resonator') for rf excitation and signal reception (19).

Vessel size imaging was performed as described previously using very small superparamagnetic iron oxide nanoparticles (VSOP; Ferropharm, Teltow, Germany; 20 μmol Fe/mouse) (18, 20).

Three-dimensional power doppler US imaging. US measurements were performed using a Vevo 770 micro-ultrasound system (VisualSonics, Toronto, Ontario, Canada) and a 40 MHz transducer (Doppler frequency: 30 MHz). The US transducer was fixed on a motor-driven unit above the animal, thereby acquiring consecutive images with a slice thickness of 300 μm. To analyze tumor volume and relative blood volume, noncontrast-enhanced power Doppler scans were performed with the following settings: power 100%, wall filter 2.5 mm/s, scan speed 2.0 mm/s. Tumors were analyzed by the Vevo 770 software as described elsewhere (17).

Indirect immunofluorescence and cryosections. Immediately after the final imaging session, animals were sacrificied and tumors were dissected for histological analysis (17). The following primary and secondary antibodies were used: rat anti-mouse CD31 (BD Biosciences, San José, CA USA), rabbit anti-mouse Ng2 (Chemicon, Temecula, CA, USA); rabbit anti-mouse smooth muscle actin (SMA) (Abcam, Cambridge, UK), guinea pig anti-mouse Vimentin (Progen, Heidelberg, Germany), guinea pig anti-mouse pan-keratin (PK) (Progen), goat-anti-mouse VEGFR-2 (Flk-1) (R&D Systems, Minneapolis, MN, USA), donkey anti-rabbit IgG (Cy2) (Dianova, Hamburg, Germany), donkey anti-rat (Cy3) (Dianova), donkey anti-guinea pig (AMKA) (Dianova) and donkey anti-goat (Cy3) (Dianova). Nuclei were stained by Hoechst/bisbenzimide (Invitrogen GmbH, Karlsruhe, Germany).

Images of fluorescence stainings were acquired and quantitatively analyzed as described previously (6).

Statistical analysis. Data analysis was performed by a non-parametric Mann-Whitney test using GraphPad Prism software version 4.03 (GraphPad, San Diego, CA, USA). $P<0.05$ was considered as significant.

Results

Necessity of human dermal fibroblasts for invasive growth of HaCaT-ras A-5RT3 cells. In OTCs, the tumor epithelium of HaCaT-ras A-5RT3 cells enlarged constantly from day 7 to

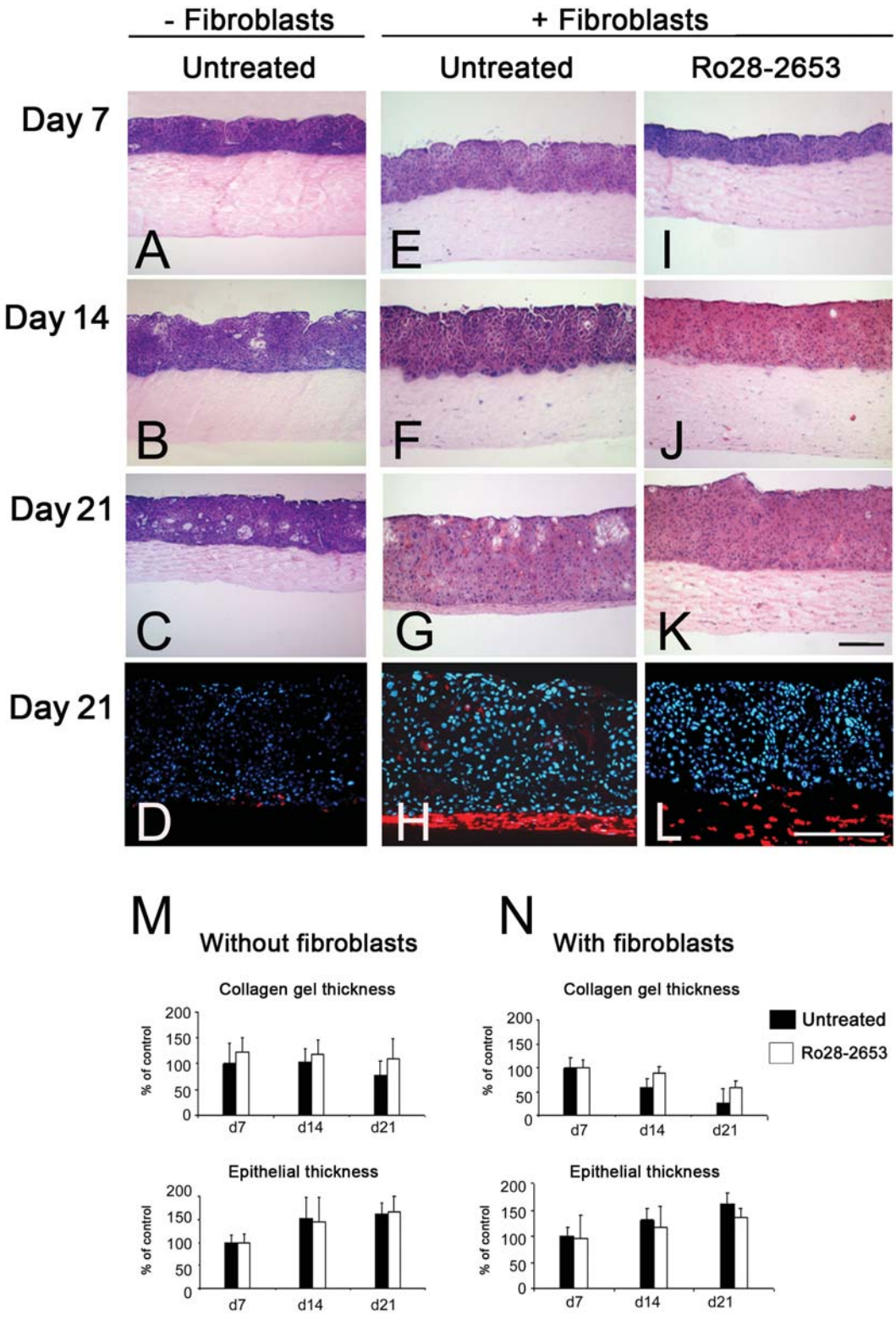

Figure 1. *The role of fibroblasts and the effect of Ro28-2653 on the maintenance of the collagen gel in OTCs. H&E staining of OTCs without (A-C) and with fibroblasts (E-G). I-K: H&E staining of Ro28-2653-treated OTCs. D, H, L: Double immunostaining of vimentin (red) and Hoechst/bisbenzimide (nuclear staining, blue) in OTCs. Scale bars: 100 μm. Quantitative analysis of collagen gel and epithelial thickness in untreated and Ro28-2653 treated OTCs without (M) and with fibroblasts (N). For comparison, untreated samples of day 7 are set to 100%. Each bar represents the mean±SD of eight independent OTCs.*

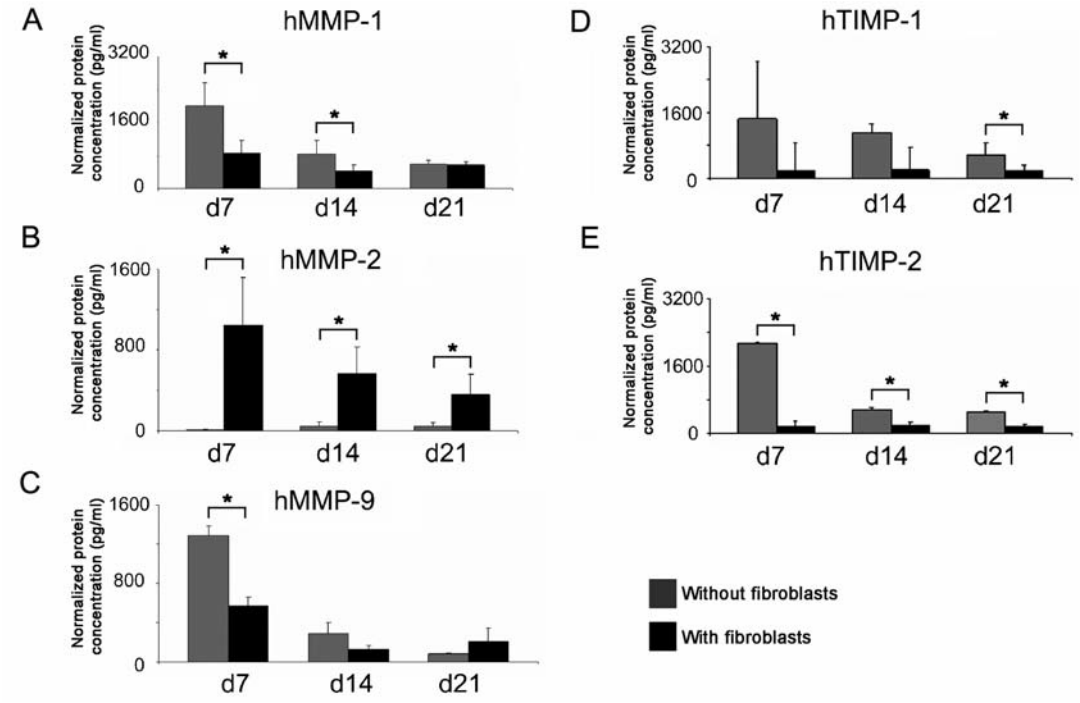

Figure 2. *Levels of hMMP-1, hMMP-2, hMMP-9, hTIMP-1 and hTIMP-2 protein in conditioned media of OTCs. MMP-1 (A), MMP-2 (B) and MMP-9 (C) protein concentration was normalized to the tumor cell number in conditioned media of OTCs with and without fibroblasts. D-E: Normalized TIMP-1 and TIMP-2 protein concentration in OTCs with and without fibroblasts. Each bar represents the mean protein concentration±SD from eight OTCs. *p<0.05.*

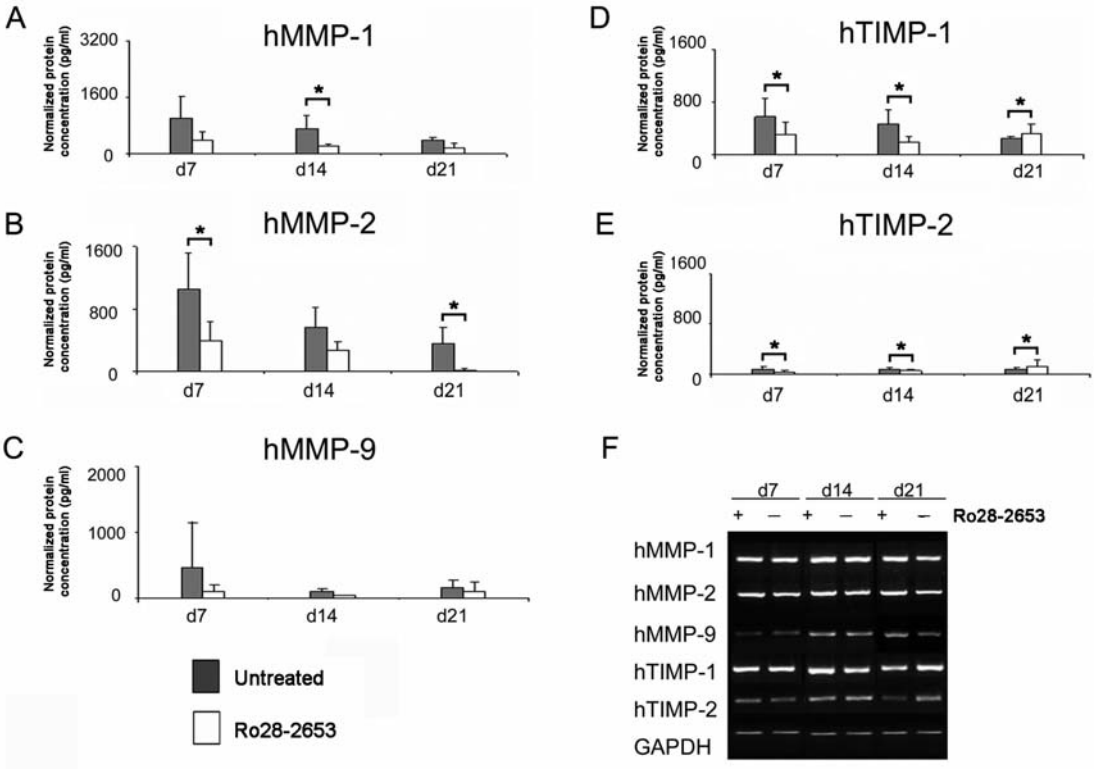

Figure 3. *Effects of MMP inhibition (Ro28-2653) on MMP-1, MMP-2, MMP-9, TIMP-1 and TIMP-2 protein and mRNA expression in OTCs with fibroblasts. Normalized MMP-1 (A), MMP-2 (B), MMP-9 (C), TIMP-1 (D) and TIMP-2 (E) protein concentration in OTCs with fibroblasts after Ro28-2953 treatment. F: RT-PCR analysis of MMP-1, MMP-2, MMP-9, TIMP-1, TIMP-2 and GAPDH mRNA expression in OTCs with fibroblasts.*

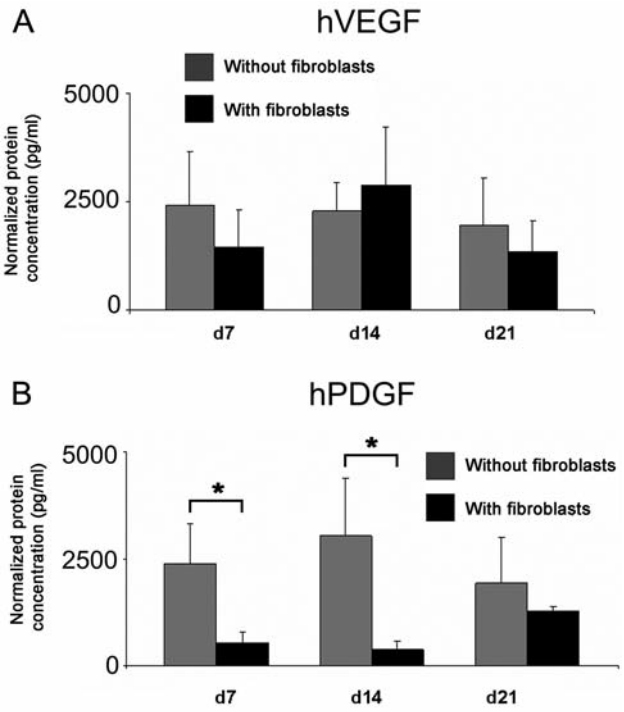

Figure 4. *VEGF-A and PDGF-BB protein expression in conditioned media of OTCs with and without fibroblasts. Normalized VEGF-A (A) and PDGF-BB (B) protein concentration in OTCs with and without fibroblasts.*

21, independently of the presence of human dermal fibroblasts. However, manifest degradation of collagen type I gel was only observed in the presence of fibroblasts (Figure 1B and F). After 3 weeks, only a thin layer of the collagen gel remained in OTCs with fibroblasts (Figure 1G).

Although the gel was almost completely replaced by the tumor epithelium, the vimentin-expressing fibroblasts were still present in the thin collagen layer beneath the epithelium, as evidenced by the condensed vimentin staining (Figure 1D, H and L).

MMP inhibition blocks gel degradation by HaCaT-ras A-5RT3 cells in OTCs. In order to analyze the impact of MMPs on tumor cell invasion, OTCs with fibroblasts were treated with the MMP inhibitor Ro28-2653, which has a high selectivity for MMP-2, MMP-9 and MMP-14, thus targeting angiogenesis- and invasion-associated MMPs. Inhibited OTCs showed a greater collagen thickness than untreated OTCs starting from day 14. No effect of MMP inhibition on the tumor epithelial thickness was visible (Figure 1).

In the absence of fibroblasts, no effect of Ro28-2653 treatment was found on collagen gel or epithelial thickness (Figure 1M), strongly suggesting that MMPs derived from fibroblasts were responsible for collagen degradation and tumor invasion.

Fibroblasts modulate the protein expression of MMPs and TIMPs. To further investigate the functional role of fibroblast derived MMPs for tumor invasion *in vitro*, the expression of MMP-1, MMP-2, MMP-9, TIMP-1 and TIMP-2 (normalized protein amount [pg]) was determined at day 7, 14 and 21 in conditioned media of OTCs with and without fibroblasts by ELISA. In the absence of fibroblasts, the maximum expression of MMP-1 (Figure 2A), MMP-9 (Figure 2C) and of TIMPs (Figure 2 D and E) was at day 7 of culture, with MMP-1 showing the highest expression level (Figure 2A). MMP-1 and MMP-9 expression was enhanced in fibroblast-free OTCs during the first two weeks of culture, whereas in the third week, MMP-1 and MMP-9 levels became comparable to these of fibroblast-containing OTCs (Figure 2A and C). TIMP-1 and TIMP-2 expression was higher in OTCs without fibroblasts at all time points (Figure 2D and E). In contrast, the expression of MMP-2 was significantly ($p<0.01$) higher in OTCs with fibroblasts at all time points analyzed (Figure 2B).

Influence of Ro28-2653 treatment on MMP and TIMP expression. In OTCs without fibroblasts, only the amounts of MMP-1 and TIMP-1 protein were reduced significantly ($p<0.05$) after MMP inhibition (data not shown).

In OTCs with fibroblasts, Ro28-2653 also significantly reduced the level of MMP-1 protein from days 7 to 14, while the mRNA level did not change significantly (Figure 3A). *MMP-2* mRNA (Figure 3F, lane 2) and protein (Figure 3B) were both reduced in treated OTCs at all time points (Figure 3B). In contrast, *MMP-9* mRNA and protein were not significantly affected by Ro28-2653 (Figure 3C and F, lane 3). *TIMP-1* protein and mRNA levels significantly decreased in treated OTCs ($p<0.05$) at day 7 and 14, but increased above that of the untreated samples at day 21 (Figure 3D and 3F, lane 4). TIMP-2 was significantly reduced ($p<0.05$) by Ro28-653 treatment on day 7 and 14, but increased above that of the untreated samples in the third week of MMP inhibition ($p<0.01$) (Figure 3E and and 3F, lane 5).

Expression of PDGF-BB and VEGF-A protein. Besides MMPs, VEGF-A and PDGF-BB are important angiogenesis-promoting factors. Since previous studies have demonstrated that tumor cell-derived PDGF-BB regulates VEGF-A expression in fibroblasts (6), we analyzed the concentration of both factors in conditioned media of OTCs. While the expression of VEGF-A was not influenced by the presence of fibroblasts (Figure 4A), PDGF-BB levels significantly increased in OTCs without fibroblasts from day 7 to 14 but became comparable after 3 weeks of culture (Figure 4B).

Ro28-2653 treatment of OTCs with and without fibroblasts reduced the amount of VEGF-A in conditioned media throughout the whole observation period compared to

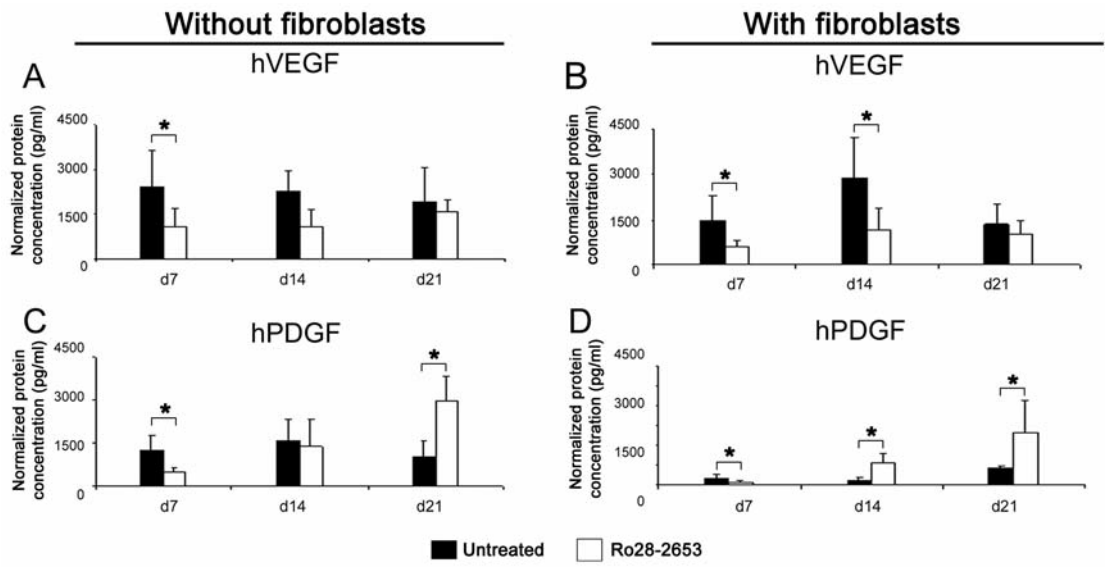

Figure 5. *Changes in VEGF-A and PDGF-BB protein levels after Ro28-2653 treatment in OTCs without (A-B) and with fibroblasts (C-D). VEGF-A (A, B) and PDGF-BB (C, D) protein expression in MMP-inhibited OTCs without (A, C) and with (B, D) fibroblasts.*

untreated samples (Figure 5A and 5B). The inhibitory effects were more prominent at day 7 and 14 ($p<0.05$) than at day 21 (Figure 5A and 5D).

The expression of PDGF-BB in fibroblast-free and fibroblast-containing OTCs was significantly reduced after treatment with Ro28-2653 at day 7 ($p<0.05$) (Figure 5C and 5D). Thereafter, Ro28-2653 induced an increase in the PDGF level compared to untreated controls, leading to significantly higher amounts at day 21 (Figure 5C and 5D).

Effects of MMP inhibition on tumor invasion, vascularization, tumor size and on the expression of VEGF-A and MMP-14 in HaCaT-ras A5RT3 tumor xenografts in vivo. Since MMP-2 was found to be crucial for tumor cell invasion *in vitro*, we used Ag3340 as a more MMP-2 specific inhibitor for *in vivo* experiments. Additionally, Ag3340 was better established for *in vivo* experiments at that time. Treatment of HaCaT-ras A-5RT3 tumor xenografts with Ag3340 for 6 days strongly reduced tumor invasion and vascularization. In contrast to the highly invasive and well-vascularized control tumors (Figure 6A, invasive tumor islets are marked by arrows), the tumor tissue was barely vascularized and partially necrotic after 6 days of treatment, and no invasive tumor islets were observed (Figure 6B, the line marks the tumor stroma border zone). The strong vimentin staining in the stroma indicated an accumulation of fibroblasts (Figure 6A and B). Interestingly, MMP inhibition also reduced the tumor size (Figure 6C). Doppler US (Figure 6C) demonstrated significantly reduced relative blood volume in treated animals (1.8±1.4%) compared to untreated ones (5.2±3.1%), confirming a strong decrease in tumor vascularization.

The mean vessel diameter (Figure 6D), analyzed by vessel size imaging with MRI, remained constant in untreated animals (day 0: 53±10 μm, day 6: 57±20 μm), but significantly increased in response to Ag3340 treatment (prior to therapy, day 0: 40±10 μm, after therapy, day 6: 70±10 μm; $p<0.05$). This suggests that MMP inhibition reduces the number of small, newly formed, immature vessels. Therefore, we determined the ratio of mature vessels compared to the total vessel density on tumor sections (Figure 6E-G) using Ng2 as a pericyte marker. Indeed, the ratio of Ng2- to CD31-positive areas was higher after MMP inhibition (treated: 4.6±2.6, untreated 3.0±1.9) (Figure 6E), demonstrating an increase in the percentage of mature vessels.

In order to analyze whether reduced angiogenesis and tumor vascularization were due to the observed effects of the MMP blockade on growth factor and MMP expression, we assessed the expression of VEGF-A in the xenotransplants as well as the expression of MMP-14, the key activator of MMP-2. In line with the *in vitro* data, Ag3340 treatment markedly reduced the expression of murine VEGF-A in the stroma of the HaCaT-ras A-5RT3 tumors (Figure 7A and B). In addition, MMP-14 protein was almost absent in the remaining vascularized parts of the treated tumors in comparison to the control tumors (Figure 7C and D, stromal areas are marked by arrows).

Discussion

Cancer development and progression are controlled by interactions between tumor and stromal cells (1-4). Activated (myo-) fibroblasts are known to support tumor

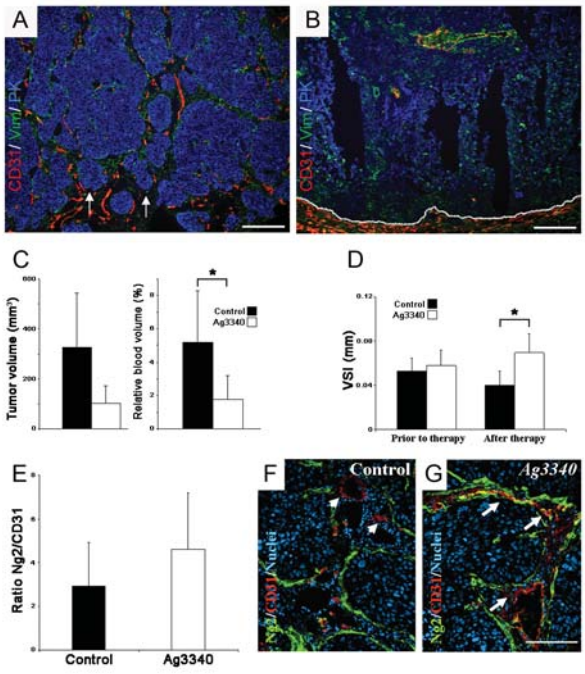

Figure 6. *Effects of the MMP inhibitor Ag3340 on tumor invasion, vascularization and size in HaCaT-ras A-5RT3 tumor xenografts. A-B: Immunostaining of CD31 (red), vimentin (green, Vim) and pan-keratin (blue, PK) demonstrates the highly invasive and vascularized control tumors (A) and the strong inhibition of tumor invasion and vascularization (B) after 6 days of treatment (invasive tumor islets are marked by arrows in A, the normalized tumor border zone is marked by a dashed line in B). Scale bar: 200 μm. C: Tumor volume and relative blood volume of treated and untreated HaCaT-ras A5RT3 xenografts as determined by high frequency ultrasound. *p<0.05. D: Mean tumor vessel diameter analyzed by vessel size imaging (MRI). *p<0.05. E: Quantitative analysis of Ng2-positive area fractions normalized to the corresponding CD31-positive area of tumor sections. F-G: Representative images of corresponding tumor sections stained by CD31 (red), Ng2 (green) and Hoechst/bisbenzimide (blue). Scale bar: 100 μm.*

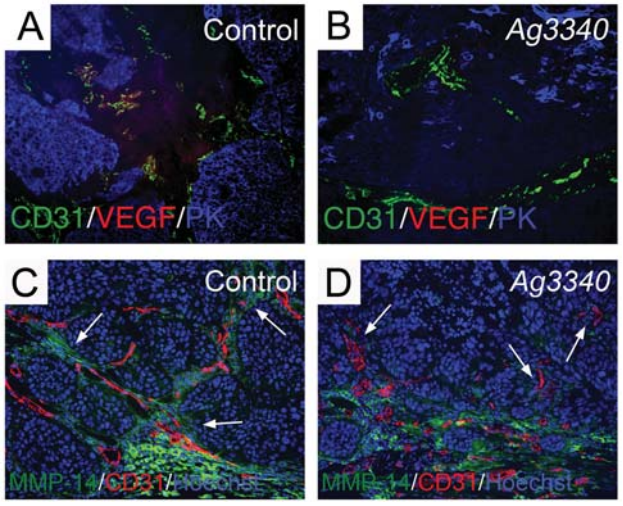

Figure 7. *Effects of Ag3340 on VEGF-A and MMP-14 protein expression in HaCaT-ras A-5RT3 tumor xenografts. A-B: Immunostaining for CD31 (green), murine VEGF-A (mVEGF-A, red) and pan-keratin (PK, blue). C-D: Immunostaining for MMP-14 (green), CD31 (red) and Hoechst (blue). Scale bar: 100 μm.*

initiation, angiogenesis and invasion through the secretion of cytokines and proteases (21-22). Nevertheless, the mechanisms of interaction between carcinoma cells and stromal fibroblasts have not yet been elucidated in detail. To assess the direct influence of fibroblasts on tumor cell growth, we used three-dimensional OTCs of highly malignant HaCaT-ras A-5RT3 cells with and without fibroblasts and investigated the expression of invasion and angiogenesis associated MMPs, TIMPs and growth factors in the absence and presence of an MMP inhibitor. Since angiogenesis as crucial pre-requisite for tumor invasion (23) cannot be mimicked in OTCs, we analyzed the effect of MMP inhibition on *s.c.* HaCaT-ras A-5RT3 xenografts *in vivo* and assessed tumor invasion, size and vascularization by non invasive imaging and histology.

In OTCs, a significant reduction in collagen gel thickness was only observed in the presence of fibroblasts, indicating their crucial contribution to tumor cell invasion. The fibroblast-dependent differences in collagen gel degradation were associated with an altered MMP expression profile. During the first two weeks of culture, the MMP-1 and MMP-9 levels were higher in OTCs without fibroblasts. This might be explained by an induction of these MMPs in tumor cells when they come into contact with the dense collagen type I matrix and start to build up an epithelium. This hypothesis is supported by the observed MMP-1 induction in normal keratinocytes on contact with collagen type I (24). At late time points, when a multilayered tumor epithelium had formed, the levels of MMP-1 and MMP-9 decreased again. Since fibroblasts crucially support the epithelial growth in OTCs by cytokine production (25), they might exert normalizing effects on MMP induction during the early growth phase. The MMP-2 protein levels were strikingly increased in conditioned media of fibroblast-containing OTCs throughout the whole observation period, demonstrating fibroblasts as potent producers of MMP-2 (26). MMP-2 is strongly expressed in malignant tumors and stromal MMP-2 promotes tumor growth in breast cancer (27, 28). Since active collagen degradation was only observed in OTCs with fibroblasts, the increased MMP-2 levels in these cultures suggest that MMP-2 secreted by fibroblasts may drive tumor cell invasion. This is supported by the lower levels of the natural MMP inhibitors TIMP-1 and TIMP-2 in fibroblast-containing OTCs.

Treatment of fibroblast-containing OTCs with the MMP inhibitor Ro28-2653 resulted in significantly lower mRNA and protein levels of MMP-1, MMP-2, TIMP-1 and TIMP-2, whereas MMP-9 expression was not affected. In week three, when most of the collagen gel was degraded, only MMP-2 levels remained significantly lower in the Ro28-2653 treated cultures with fibroblasts, while TIMP-1 and TIMP-2 expression even increased. This substantiates the notion that fibroblast-derived MMP-2 is the main mediator of collagen degradation and of tumor cell invasion in the OTCs. The higher TIMP levels after Ro28-2653 treatment of fibroblast-containing OTCs correlate to the enhanced TIMP levels in OTCs without fibroblasts (showing no obvious collagen degradation). However, the mechanism for the Ro28-2653-mediated TIMP up-regulation remains unknown.

Next, we assessed whether the presence or absence of fibroblasts also had an influence on the expression of the prominent angiogenic factors VEGF-A and PDGF-BB. Whereas VEGF-A expression was similar in OTCs with or without fibroblasts, the amount of PDGF-BB was significantly higher in fibroblast-free OTCs during the first two weeks of culture and this decreased to the control level at week three. Thus, the kinetics of PDGF-BB expression were similar to those of MMP-1 in fibroblast-free OTCs and might be explained by a wound-like reaction at the initial growth phase, with MMP-1 and PDGF-BB facilitating the epithelialization of the gel in the absence of fibroblasts (6, 29). Interestingly, the MMP inhibitor Ro28-2653 did not only affect MMP expression, but also significantly reduced VEGF-A protein expression during the first two weeks of treatment. In contrast, the PDGF-BB levels continuously increased in response to the MMP inhibition. This might be explained by an inhibitory effect of high PDGF-BB levels on VEGF-A expression by fibroblasts, as previously described (6). Since PDGF-BB additionally promotes pericyte recruitment and vessel maturation (6), we investigated the effects of MMP inhibition not only on tumor growth and invasion, but also on the vascularization of HaCaT-ras A-5RT3 *s.c.* xenografts *in vivo*. We used the MMP inhibitor Ag3340, which has an even higher affinity for MMP-2, the invasion-associated MMP, in the OTCs. Comparably to the reduced collagen degradation seen *in vitro*, we observed a strong inhibition of tumor invasion after 6 days of Ag3340 treatment in the xenografts *in vivo*. The intense vimentin staining in the intratumoral stromal strands of the treated and untreated tumors strongly suggested that fibroblasts might promote tumor invasion in the controls. In addition, tumor vascularization was strongly inhibited. This was substantiated by Doppler US, demonstrating a lower relative blood volume in the treated HaCaT-ras A-5RT3 xenografts. The decreased tumor volume of the treated HaCaT-ras A-5RT3 tumors, as measured by us, demonstrated that MMP inhibition even induced tumor shrinkage. On the other hand, the mean vessel size assessed by MRI increased significantly, strongly suggesting that Ag3340 caused the regression of small, newly formed immature vessels. Indeed, analysis of vessel maturation by immunostaining with the pericyte marker Ng2 revealed an increase in the fraction of Ng2-positive, mature vessels in the treated tumors. In addition, Ag3340 almost completely reduced the expression of host VEGF-A and of MMP-14, the key activator of MMP-2. Thus, we observed a similar correlation between the inhibition of invasion and the reduction of MMP and VEGF-A in xenografts and OTCs treated with an MMP inhibitor.

In summary, human dermal fibroblasts play an essential role for tumor invasion, most probably mediated *via* MMP-2. Moreover, the data reveal a complex interplay between MMPs, TIMPs and growth factors such as VEGF-A and PDGF-BB that regulate tumor invasion and vascularization, as well as vessel maturation and vessel function.

Acknowledgements

Our thanks go to Silke Haid, Renate Bangert, and H. Steinbauer for their excellent technical assistance. We also thank Pfizer Inc. for kindly providing samples of the therapeutic drug Ag3340, and Roche Diagnostics GmbH for Ro28-2653. This work was supported by a grant from the 6th EU Framework for an integrated project in the European Cancer Proteases Consortium (EUCPC), project #: LSHC-CT- 2003-503297.

References

1 Liotta LA and Kohn EC: The microenvironment of the tumour–host interface. Nature *411*: 375-379, 2001.

2 Dong-Le Bourhis X, Berthois Y, Millot G, Degeorges A, Sylvi M, Martin PM and Calvo F: Effect of stromal and epithelial cells derived from normal and tumorous breast tissue on the proliferation of human breast cancer cell lines in co-culture. Int J Cancer *71*: 42-48, 1997.

3 Olumi AF, Grossfeld GD, Hayward SW, Carroll PR, Tlsty TD and Cunha GR: Carcinoma-associated fibroblasts direct tumor progression of initiated human prostatic epithelium. Cancer Res *59*: 5002-5011, 1999.

4 Kalluri R and Zeisberg M: Fibroblasts in cancer. Nat Rev Cancer *6*: 392-401, 2006.

5 Ferrara N, Gerber HP and LeCouter J: The biology of VEGF and its receptors. Nat Med *6*: 669-676, 2003.

6 Lederle W, Stark HJ, Skobe M, Fusenig NE and Mueller MM: Platelet-derived growth factor-BB controls epithelial tumor phenotype by differential growth factor regulation in stromal cells. Am J Pathol *169*: 1767-1783, 2006.

7 Kitadai Y, Sasaki T, Kuwai T, Nakamura T, Bucana CD, Hamilton SR and Fidler IJ: Expression of activated platelet-derived growth factor receptor in stromal cells of human colon carcinomas is associated with metastatic potential. Int J Cancer *119*: 2567-2574, 2006.

8 Rundhaug JE: Matrix metalloproteinases, angiogenesis, and cancer. Clin Cancer Res *9*: 551-554, 2003.

9 Medina C, Videla S, Radomski A, Radomski MW, Antolín M, Guarner F, Vilaseca J, Salas A and Malagelada JR: Increased activity and expression of matrix metalloproteinase-9 in a rat model of distal colitis. Am J Physiol Gastrointest Liver Physiol *284*: 116-122, 2003.
10 Fang J, Shing Y, Wiederschain D, Yan L, Butterfield C, Jackson G, Harper J, Tamvakopoulos G and Moses MA: Matrix metalloproteinase-2 is required for the switch to the angiogenic phenotype in a tumor model. Proc Natl Acad Sci USA *97*: 3884-3889, 2000.
11 Egeblad M and Werb Z: New functions for the matrix metalloproteinases in cancer progression. Nat Rev Cancer *2*: 161-174, 2002.
12 Coussens LM, Fingleton B and Matrisian LM: Matrix metalloproteinase inhibitors and cancer: Trails and tribulations. Science *295*: 2387-2392, 2002.
13 Grams F, Brandstetter H, D'Alò S, Geppert D, Krell HW, Leinert H, Livi V, Menta E, Oliva A, Zimmermann G, Gram F, Brandstetter H, D'Alò S, Geppert D, Krell HW, Leinert H, Livi VMenta E, Oliva A and Zimmermann G: Pyrimidine-2,4,6-triones: a new effective and selective class of matrix metalloproteinase inhibitors. Biol Chem *382*: 1277-1285, 2001.
14 Lein M, Jung K, Ortel B, Stephan C, Rothaug W, Juchem R, Johannsen M, Deger S, Schnorr D, Loening S and Krell HW: The new synthetic matrix metalloproteinase inhibitor (Roche 28-2653) reduces tumor growth and prolongs survival in a prostate cancer standard rat model. Oncogene *21*: 2089-2096, 2002.
15 Vosseler S, Mirancea N, Bohlen P, Mueller MM and Fusenig NE: Angiogenesis inhibition by vascular endothelial growth factor receptor-2 blockade reduces stromal matrix metalloproteinase expression, normalizes stromal tissue, and reverts epithelial tumor phenotype in surface heterotransplants. Cancer Res *65*: 1294-1305, 2005.
16 Breitkreutz D, Mirancea N, Schmidt C, Beck R, Werner U, Stark HJ, Gerl M and Fusenig NE: Inhibition of basement membrane formation by a nidogen-binding laminin gamma1-chain fragment in human skin-organotypic cocultures. J Cell Sci *15*: 2611-2622, 2004.
17 Palmowski M, Huppert J, Hauff P, Reinhardt M, Schreiner K, Socher MA, Hallscheidt P, Kauffmann GW, Semmler W and Kiessling F: Vessel fractions in tumor xenografts depicted by flow- or contrast-sensitive 3D high-frequency Doppler ultrasound respond differently to multispecific tyrosine kinase receptor inhibition. Cancer Res *68*: 7042-7049, 2008.
18 Zwick S, Strecker R, Kiselev V, Gall P, Huppert J, Palmowski M, Lederle W, Woenne EC, Hengerer A, Taupitz M, Semmler W and Kiessling F: Assessment of vascular remodeling under antiangiogenic therapy using DCE-MRI and vessel size imaging. J Magn Reson Imaging *29*: 1125-1133, 2009.
19 Zhang C, Jugold M, Woenne EC, Lammers T, Morgenstern B, Mueller MM, Zentgraf H, Bock M, Eisenhut M, Semmler W and Kiessling F: Specific targeting of tumor angiogenesis by RGD-conjugated ultrasmall superparamagnetic iron oxide particles using a clinical 1.5-T magnetic resonance scanner. Cancer Res *67*: 1555-1562, 2007.
20 Troprès I, Grimault S, Vaeth A, Grillon E, Julien C, Payen JF, Lamalle L and Décorps M: Vessel size imaging. Magn Reson Med *45*: 397-408, 2001.
21 Beacham DA and Cukierman E: Stromagenesis: the changing face of fibroblastic microenvironments during tumor progression. Semin Cancer Biol *15*: 329-341, 2005.
22 De Wever O, Demetter P, Mareel M and Bracke M: Stromal myofibroblasts are drivers of invasive cancer growth. Int J Cancer *15*: 2229-2238, 2008.
23 Carmeliet P and Jain RK: Angiogenesis in cancer and other diseases. Nature *407*: 249-257, 2000.
24 Pilcher BK, Dumin JA, Sudbeck BD, Krane SM, Welgus HG and Parks WC: The activity of collagenase-1 is required for keratinocyte migration on a collagen type I matrix. J Cell Biol *37*: 1445-1457, 1997.
25 Szabowski A, Maas-Szabowski N, Andrecht S, Kolbus A, Schorpp-Kistner M, Fusenig NE and Angel P: c-Jun and JunB antagonistically control cytokine-regulated mesenchymal-epidermal interaction in skin. Cell *103*: 745-755, 2000.
26 Ingvarsen S, Madsen DH, Hillig T, Lund LR, Holmbeck K, Behrendt N and Engelholm LH: Dimerization of endogenous MT1-MMP is a regulatory step in the activation of the 72-kDa gelatinase MMP-2 on fibroblasts and fibrosarcoma cells. Biol Chem *389*: 943-953, 2008.
27 Shah FD, Shukla SN, Shah PM, Shukla HK and Patel PS: Clinical significance of matrix metalloproteinase 2 and 9 in breast cancer. Indian J Cancer *246*: 194-202, 2009.
28 Taniwaki K, Fukamachi H, Komori K, Ohtake Y, Nonaka T, Sakamoto T, Shiomi T, Okada Y, Itoh T, Itohara S, Seiki M and Yana I: Stroma-derived matrix metalloproteinase (MMP)-2 promotes membrane type 1-MMP-dependent tumor growth in mice. Cancer Res *67*: 4311-3419, 2007.
29 Barrientos S, Stojadinovic O, Golinko MS, Brem H and Tomic-Canic M: Growth factors and cytokines in wound healing. Wound Repair Regen *16*: 585-601, 2008.

Received November 18, 2009
Accepted January 12, 2010